# Statistical Relaxation under Nonturbulent Chaotic Flows: Non-Gaussian High-Stretch Tails of Finite-Time Lyapunov Exponent Distributions

Darin Beigie,[1] Anthony Leonard,[2] and Stephen Wiggins[3]
[1]*Center for Applied Mathematics and Theory Center, Cornell University, Ithaca, New York 14853*
[2]*Graduate Aeronautical Laboratories, California Institute of Technology, Pasadena, California 91125*
[3]*Department of Applied Mechanics, California Institute of Technology, Pasadena, California 91125*
(Received 23 September 1992)

We observe that high-stretch tails of finite-time Lyapunov exponent distributions associated with interfaces evolving under a class of nonturbulent chaotic flows can range from essentially Gaussian tails to nearly exponential tails, and show that the non-Gaussian deviations can have a significant effect on interfacial evolution. This observation motivates new insight into stretch processes under chaotic flows.

PACS numbers: 47.10.+g, 05.45.+b

We investigate probability distributions of finite-time Lyapunov exponents (or simply *stretch distributions*) associated with interfaces evolving within the chaotic tangles of 2D time-periodic vector fields. Such statistics are relevant, for example, to the mixing process in fluid flows, where the stretching of an interface between two species affects the rate of mixing, and to kinematic dynamo phenomena, where the stretching of fluid elements affects magnetic field amplification. In contrast to previous studies of stretch statistics associated with chaotic flows [1–9], we focus explicitly on the high-stretch tails of these distributions, which are relevant for several reasons. First, though the high-stretch tails correspond to small probability values, we find they can play a significant role in interfacial stretching. Second, for incompressible flows these tails correspond to the limit of small spatial scales (small striation width), and thus have direct impact on the multifractal characteristics of passive scalars in the small-striation-width regime. Third, the turbulence community has shown significant recent interest in probability distribution function (PDF) tails [10–16], and in a related context fractal and multifractal characterizations associated with these distributions (e.g., see Sreenivasan [17] and references therein), and it should be of interest to understand distribution tails associated with nonturbulent chaotic flows. We thus perform a high-resolution numerical study of these high-stretch tails by implementing a dynamic point insertion scheme to maintain good interfacial covering. Such a scheme allows one to determine tail behavior right up to the maximum stretch in the distribution. We observe that high-stretch tails can take on a range of behavior, depending on the system at hand, varying from essentially Gaussian to nearly exponential, and show that the non-Gaussian deviations can play a significant role in interfacial evolution. Such an observation indicates the need for sufficiently high-resolution experiments to capture tail behavior when studying stretch statistics associated with chaotic flows. The range of high-stretch tail statistics is understandable in the context of our recent analysis of interfacial stretching in chaotic tangles, which shows via a symbolic dynamics construction how, though one can view the stretch process in chaotic tangles in terms of products of weakly correlated events, these events can involve a variety of stretch scales, spatial scales, and temporal scales, allowing for a range of tail statistics [18,19].

*Two chaotic flows.*— We consider interfacial stretching within 2D chaotic tangles, focusing for illustration on two well-studied oscillating vortex pair flows induced by (i) a pair of equal and opposite point vortices and (ii) a pair of identical point vortices oscillating periodically in response to a time-periodic straining field [18–20]. We henceforth refer to these two flows as the open and closed flow, respectively, whose stream functions, in the comoving and corotating frames, respectively, can be written as

$$\psi_{o,c} = -\frac{\Gamma}{4\pi}\{\ln[(x-x_v)^2+(y-y_v)^2] \mp \ln[(x\mp x_v)^2+(y+y_v)^2]\} + \varepsilon xy\sin(2\pi t) + \psi_{\text{tr}}, \tag{1}$$

where $(x_v, y_v)$ represents the spatial coordinates of one of the vortices in the pair, $\Gamma$ is the magnitude of circulation associated with each vortex, and $\psi_{\text{tr}}$ is the stream function associated with transforming to the comoving and corotating frame (which is easily determined from the flows) [18–20]. It is well understood that in these periodically oscillating vortex flows one obtains *chaotic tangles* (regions in physical space where there is chaotic motion) [18–20]. The boundaries of these tangles are defined by the global stable and unstable manifolds of hyperbolic fixed points in a 2D Poincaré section $\Sigma$, which represents the fluid at discrete sample times $t = n \in \mathbb{Z}$ (see Fig. 1). We consider a particularly relevant interface defined by the segment of the unstable manifold associated with one of the so-called *turnstile lobes* [18,19], as shown in Fig. 1. As the interface evolves under the chaotic flow, it exhibits the generic behavior of repeated stretching, folding, and wrapping around itself in a horseshoe fashion, its arclength growing exponentially in time [18,19]. Recent at-

 

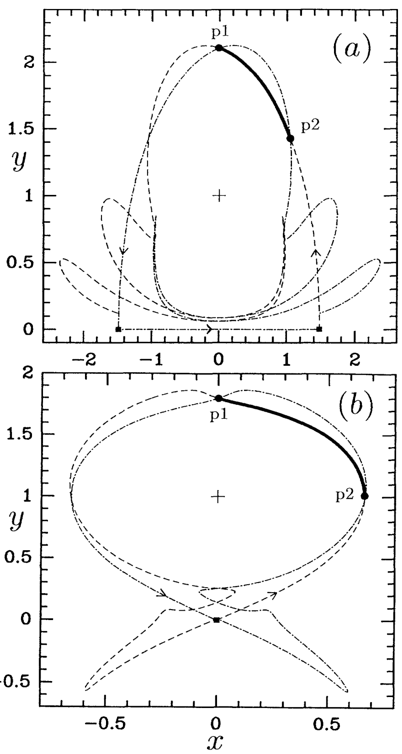


FIG. 1. Segments of stable (dash-dotted) and unstable (dashed) manifolds of hyperbolic fixed points (solid squares) in $\Sigma$, and our chosen interface (solid line) for the (a) open and (b) closed flow. The vortices are at $(x,y)=(0,\pm 1)$ at $t=n\in\mathbb{Z}$, with magnitude of circulation $\Gamma=0.4(2\pi)^2$ and (a) $\varepsilon=0.085\times 2\pi$, (b) $\varepsilon=0.02\times 2\pi$.

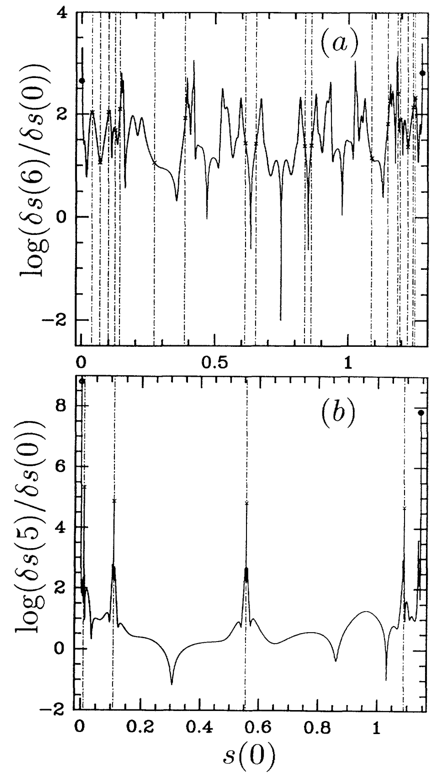


FIG. 2. Plots of *stretch profiles* for (a) the open flow at $n=6$ and (b) the closed flow at $n=5$, where $s(n)$ denotes arclength along the interface (increasing from $p1$ to $p2$). The stretch profiles are plots of *stretch* $\delta s(n)/\delta s(0)$ on a common logarithmic scale vs initial arclength of the interface $s(0)$.

tention has been given to the statistics associated with ensembles of infinitesimal line elements (or area elements) distributed along such an interface (or area of interest) [1-9]. Recognizing that stretch processes under chaotic flows can be characterized as products of weakly correlated events, a basic finding has been that the stretch distributions are well described as Gaussian near the maximum, but no explicit and detailed study of the high-stretch tails has been made. Our recent symbolic dynamics description for interfacial evolution in chaotic tangles explicitly portrays the variety of stretch scales, spatial scales, and temporal scales associated with these weakly correlated events (each "event" can be thought of as a revolution about the chaotic tangle) [18,19], and we thus expect the possibility of a variety of tail statistics. A way to appreciate this variety is to consider interfacial *stretch profiles*, i.e., plots of stretch versus initial arclength along the interface at a given sample time (see Fig. 2). The open- and closed-flow profiles are markedly different as a simple consequence of different flow geometry and flow parameters (e.g., the hyperbolic fixed point's unstable eigenvalue is significantly higher in the closed-flow tangle, and there is an additional hyperbolic fixed point in the open-flow tangle), which determine the nonuniformity of the profiles [18,19]. The closed flow exhibits a highly nonuniform stretch profile with isolated sharp peaks of very large stretch values localized over very small initial interfacial arclengths. Additionally, the vertical dashed lines in Fig. 2 indicate points on the interface which intersect the stable manifold, and hence asymptotically approach a hyperbolic fixed point. Therefore as one gets closer to these points along the interface, the corresponding revolution time around the chaotic tangle goes to infinity. Hence the closed-flow profile contains isolated sharp peaks of good stretching associated with very small spatial scales and large temporal scales. In contrast, the open-flow profile is substantially more uniform, and has, loosely speaking, evolved from a more even mix of scales [18,19]. It seems plausible that the tail statistics are qualitatively different for the two flows.

*Distributions of finite-time Lyapunov exponents.* —Given an ensemble of infinitesimal line elements distributed along an interface, let $P(\lambda(n);n)$ denote the probability distribution at the $n$th cycle ($t=n\in\mathbb{Z}$) of the finite-time Lyapunov exponent $\lambda(n)\equiv\ln[\delta s(n)/\delta s(0)]/n$, where $\delta s(n)$ denotes the length at the $n$th cycle of an infinitesimal line segment that originates along our interface. Studies of finite-time Lyapunov exponent distributions conventionally monitor a fixed number of particles, and thus approximate $P(\lambda(n);n)$ as the percentage of particles per bin width $\delta\lambda$ at a given $\lambda(n)$ bin. In contrast, we employ a point insertion scheme that maintains the covering of our interface to within a certain width (chosen to be about 1% of the mean vortex separation, a stringent criterion). When neighboring points separate beyond a cutoff, we insert a new point between them along the interface, its associated stretch history interpolated from the two neighboring points (accurate for a dense enough interfacial grid), and adjust the initial arclengths of the line segments associated with the inserted and neighboring points. The result at the $n$th cycle is thus a partitioning of the interface, of total length $s_{\mathrm{tot}}(n)$, into a set of small line elements $\{\delta s_i(n)|\sum_i \delta s_i(n) = s_{\mathrm{tot}}(n)\}$, each of which has a specified *stretch* $\delta s_i(n)/\delta s_i(0)$ and initial arclength $\delta s_i(0)$. The stretch and initial arclength can vary greatly along the interface. Hence, an improved approximation of $P(\lambda(n);n)$ is given by the *percentage of the interface's initial arclength per bin width* $\delta\lambda$ *in the* $\lambda(n)$ *bin*:

$$P(\lambda(n);n) = \frac{1}{\delta\lambda} \sum_{\substack{i \\ \lambda_i(n) \in \lambda(n)\mathrm{bin}}} \frac{\delta s_i(0)}{s_{\mathrm{tot}}(0)}, \qquad (2)$$

where $\lambda_i(n)$ is the finite-time Lyapunov exponent associated with the $i$th line element. Our prescription is similar to a fixed particle-number scheme with appropriately weighted initial particle separations, and we checked our results against this alternative scheme to confirm negligible point insertion error.

We find for our class of chaotic tangles that high-stretch tails of finite-time Lyapunov exponent distributions can range from essentially Gaussian to nearly exponential. This range of behavior is illustrated by plotting the distributions on a logarithmic scale and then scaling the vertical axis with division by $n$ (see Fig. 3). The open-flow tail, which corresponds to a more uniform stretch profile, is essentially Gaussian by $n=10$. The closed-flow tail, which corresponds to a much more nonuniform stretch profile with isolated sharp peaks of good stretching localized over small spatial scales and large temporal scales, appears to be nearly exponential by $n=10$. Hence stretch profiles of differing nonuniformities can engender high-stretch tails of different character; in particular, highly nonuniform stretch profiles can entail significantly non-Gaussian tails. Note that the closed-flow non-Gaussian deviations are significant only at small probabilities, accompanied by a sizable Gaussian hump, thus requiring a high-resolution experiment for detection. By $n=10$ the transient behavior of the scaled distributions has decayed considerably (but not completely), so that, for example, the $n=9$ and $n=10$ distributions lie essentially on top of one another. One can thus confidently claim in the closed-flow example significant

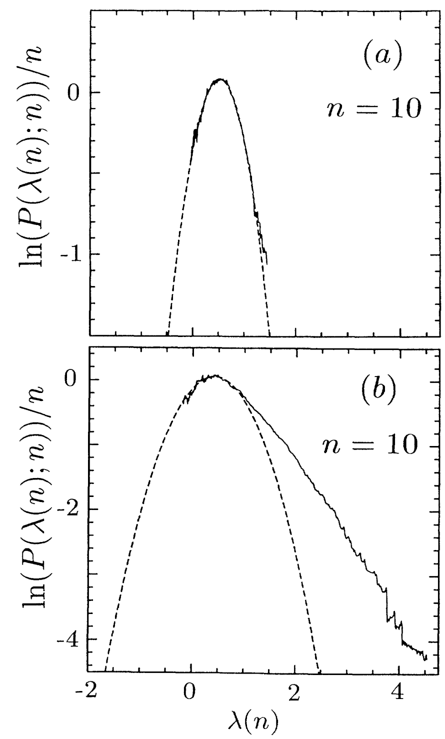


FIG. 3. Stretch distributions (solid lines) of (a) the open flow and (b) the closed flow at $n=10$. The dashed lines are Gaussian approximations, defined by having the same mean and standard deviation as the actual distributions.

non-Gaussian behavior on short and medium time scales, and it seems plausible this behavior persists asymptotically under the present scaling. Though one might be tempted to draw a definitive conclusion about the asymptotic distribution, we avoid this temptation for two basic reasons. First, an appearance of convergence can be deceptive in the context of stretch distributions, for the distributions can vary slowly over long time scales. For example, because all particles on the open-flow interface (except those which intersect the stable manifold) will end up infinitely far away from the hyperbolic fixed points, the maximum of the open-flow distribution asymptotically approaches $\lambda=0$ very slowly, and asymmetries in the distribution can slowly set in. Hence, comparing a few successive iterates for convergence can be meaningless in the context of distributions. Second, asymptotic results can depend on the choice of scaling. Our scaling via contraction of the vertical scale (dividing by $n$) is consistent with that of previous investigators [1,5] (we neglect a small transient term that some choose to keep in the scaling, e.g., see Ref. [5]). There are, of course, other possible scalings, such as the one employed in the central limit theorem, where one adjusts the horizontal scale. For example, here we could expand the horizontal scale via $\lambda(n) \rightarrow \sqrt{n}[\lambda(n) - \mu(n)]$, with $\mu(n)$

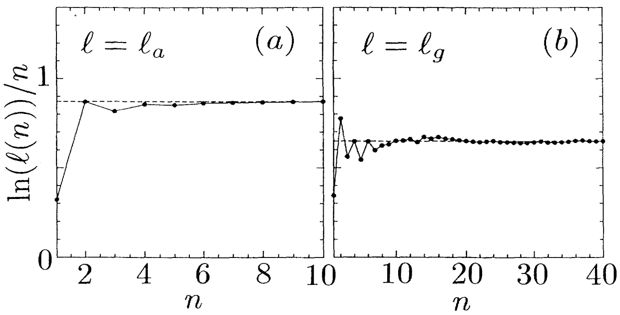


FIG. 4. Exponents associated with the growth rate of the closed-flow interfacial length. Note that the computation of $l_g(n)$ is performed over forty cycles to ensure convergence. This computation is performed with a *fixed* number of points; we verified that it does not affect the statistics associated with the Gaussian approximation $l_g(n)$ (since ignoring the high-stretch tail does not significantly alter the Gaussian approximation).

the mean of the distribution. Different scalings can give different asymptotic results; for example, a binomial distribution asymptotically approaches a Gaussian over any finite interval of its domain under the above horizontal scaling, but not under the previous vertical scaling. This horizontal scaling result (in keeping with the central limit theorem) is caused by pushing any tail deviations out to infinity, a wise scaling if one wishes to ignore vanishingly small probability values. However, in the context of stretching, it is not obvious that we wish to scale these deviations away, since small probability values are associated with large stretch values. Hence the vertical scaling is useful, and we are additionally motivated to study the effects of tail deviations in a scaling-independent framework.

*Asymptotic, scaling-independent result.*— Since the non-Gaussian deviations associated with the high-stretch tail are also associated with small probability values, we need to ask whether they can have a significant effect on the evolution of our interface. This question can be studied in a simple setting that exploits rapid convergence of a single scalar quantity, the exponent associated with the growth rate of the total length of the interface. Let $l_a(n)$ denote the total length of the *actual interface*, and $l_g(n)$ denote the total length of the *interface whose stretch statistics are described by the corresponding Gaussian approximation.* A measure of the relevance of the non-Gaussian deviations is thus the length ratio $l_g(n)/l_a(n)$. For the open-flow interface the values of $\ln[l_a(n)]/n$ and $\ln[l_g(n)]/n$ are essentially equal over the short-time calculation (up to $n=11$), as one would expect from Fig. 3(a); hence, one cannot easily conclude that any non-Gaussian deviations are significant. For the closed flow, however, Figs. 4(a) and 4(b) indicate for $l_a(n)$ and $l_g(n)$ fairly rapid convergence to different stretch rates, indicating rapid convergence of the length ratio to a time dependence

$$l_g(n)/l_a(n) \sim e^{-0.22n}. \tag{3}$$

Hence it appears that the length ratio asymptotically approaches zero, giving a strong indication in a *scaling-independent* context of the relevance of the non-Gaussian tail in the evolution of the closed-flow interface.

In conclusion, we find that high-stretch tails of finite-time Lyapunov exponent distributions associated with interfaces evolving under a class of nonturbulent chaotic flows take on a range of statistics, from essentially Gaussian to nearly exponential, and that the non-Gaussian deviations can play a significant role in interfacial stretching. A dynamic point insertion scheme allows us to explore stretch statistics with a truly 1D probe, rather than a collection of points, thus affording a high-resolution study of tail behavior right up to the maximum stretch. The range of high-stretch statistics is a consequence of the variety of stretch processes that can occur in chaotic tangles [18,19]; in particular, significantly nonuniform interfacial stretch profiles were seen here to engender significantly non-Gaussian high-stretch tails.

This material is based upon work supported by the Air Force Office of Scientific Research, the National Science Foundation, and the Office of Naval Research.


[1] P. Grassberger, R. Badii, and A. Politi, J. Stat. Phys. **51**, 135 (1988).
[2] M. A. Sepúlveda, R. Badii, and E. Pollak, Phys. Rev. Lett. **63**, 1226 (1989).
[3] T. Horita *et al.*, Prog. Theor. Phys. **83**, 1065 (1990).
[4] F. J. Muzzio, P. D. Swanson, and J. M. Ottino, Phys. Fluids A **3**, 822 (1991).
[5] F. Vărosi, T. M. Antonsen, Jr., and E. Ott, Phys. Fluids A **3**, 1017 (1991).
[6] R. T. Pierrehumbert, Phys. Fluids A **3**, 1250 (1991).
[7] H. D. I. Abarbanel, R. Brown, and M. B. Kennel, J. Nonlinear Sci. **1**, 175 (1991).
[8] J. M. Finn and E. Ott, Phys. Fluids **31**, 2992 (1988).
[9] E. Ott and T. M. Antonsen, Jr., Phys. Rev. A **39**, 3660 (1989).
[10] S. Balachandar and L. Sirovich, Phys. Fluids A **3**, 919 (1991).
[11] A. Vincent and M. Meneguzzi, J. Fluid Mech. **225**, 1 (1991).
[12] Z. She and S. A. Orszag, Phys. Rev. Lett. **66**, 1701 (1991).
[13] R. Benzi *et al.*, Phys. Rev. Lett. **67**, 2299 (1991).
[14] J. P. Gollub *et al.*, Phys. Rev. Lett. **67**, 3507 (1991).
[15] E. S. C. Ching, Phys. Rev. A **44**, 3622 (1992).
[16] P. Kailasnath, K. R. Sreenivasan, and G. Stolovitzky, Phys. Rev. Lett. **68**, 2766 (1992).
[17] K. R. Sreenivasan, Annu. Rev. Fluid Mech. **23**, 539 (1991).
[18] D. Beigie, A. Leonard, and S. Wiggins, Phys. Fluids A **3**, 1039 (1991).
[19] D. Beigie, Ph.D. thesis, Caltech (1992).
[20] V. Rom-Kedar, A. Leonard, and S. Wiggins, J. Fluid Mech. **214**, 347 (1990).